Available online at www.sciencedirect.com
SCIENCE DIRECT
Journal of Sound and Vibration 297 (2006) 55–71
JOURNAL OF SOUND AND VIBRATION
www.elsevier.com/locate/jsvi

Imposing points of zero displacements and zero slopes along any linear structure during harmonic excitations

Philip D. Cha*, Xiang Zhou[1]

Department of Engineering, Harvey Mudd College, Claremont, CA 91711, USA

Received 22 July 2005; received in revised form 2 February 2006; accepted 15 March 2006
Available online 5 June 2006

Abstract

Undamped oscillators are often employed as vibration absorbers to minimize excess vibration in structural systems. In this paper, undamped sprung masses and rotational oscillators are used to impose points of zero displacements and zero slopes for an arbitrarily supported linear structure during forced harmonic excitations. For convenience, such points are referred to as fixed nodes. When the sprung mass and rotational oscillator attachment locations and the fixed node locations coincide (or collocated), it is always possible to select the sprung mass and rotational oscillator parameters such that multiple fixed nodes are induced at any desired locations along the structure for any excitation frequency. When the attachment and the fixed node locations are not collocated (or non-collocated), however, it is only possible to induce nodes at certain locations along the elastic structure for a given driving frequency. Moreover, when the desired fixed node locations are closely spaced, it is possible to specify a region of nearly zero amplitudes for a particular driving frequency, thus drastically reducing the vibrational level in that segment of the structure. An iterative scheme is proposed that quickly leads to a set of theoretically feasible oscillator parameters that can be used to induce fixed nodes anywhere along the linear structure. Numerical case studies are performed and they validated the proposed scheme of imposing points of zero displacements and zero slopes.

1. Introduction

Attaching properly tuned vibration absorbers to a given structure for the purpose of eliminating excess vibration has been studied by many different authors over the years, and hence only a few selected references are given here. Jacquot [1] proposed a method to give the optimal dynamic vibration absorber parameters in order to eliminate the undesirable vibration in Euler–Bernoulli beams under sinusoidal excitation. However, the applicability of his method was limited in that only a single mode for the beam was employed when applying the assumed-modes method. Özgüven and Çandir [2] developed a general approach to give the optimal dynamic vibration absorber parameters to suppress any two resonances. They used the assumed-modes approach to calculate the response of the system to a concentrated harmonic excitation, and performed

*Corresponding author. Fax: +1 909 621 8967.
E-mail address: philip_cha@hmc.edu (P.D. Cha).
[1]School of Aerospace, Tsinghua University, Beijing 100084, China.

0022-460X/$ - see front matter © 2006 Elsevier Ltd. All rights reserved.
doi:10.1016/j.jsv.2006.03.032

an optimization to minimize the maximum response in any desired mode. Manikanahally and Crocker [3] employed vibration absorbers to suppress any number of significant modes. For a chosen mass, optimization of the stiffness and damping parameters of each absorber was performed to minimize the dynamic response corresponding to the resonance frequency at which the absorbers are tuned to operate. The method was successfully applied to a space structure modeled as a mass-loaded free–free beam that is under a single localized harmonic excitation. Keltie and Cheng [4] investigated the effects of point masses on the structural response of a finite beam, and proposed a technique to determine the mass locations for the purpose of reducing the vibration level at any arbitrary location on a structure. In their optimization algorithm, they used only the mass locations as the design variables. Alsaif and Foda [5] employed the dynamic Green function to determine the optimum values of masses and/or springs and their locations along a beam for the purpose of confining the vibration to an arbitrary location. The masses are rigidly attached to the beam, and the springs are grounded at one end. While the algorithm they used is exact, direct and elegant, the approach can only be applied when the Green function for the system is readily available. Zuo and Nayfeh [6] proposed a technique based on the descent-subgradient method to maximize the minimum damping of modes in a prescribed frequency range for multiple-degrees-of-freedom tuned-mass systems. The experimental results in which a two-degrees-of-freedom tuned-mass system is optimized to damp the first two modes of a free–free beam were presented to validate the proposed method. Yaman and Sen [7] investigated the effectiveness of a pendulum-type passive vibration absorber attached to a flexible beam that has a single-degree-of-freedom and is subjected to a sinusoidal base excitation. They determined the optimal orientation of the absorber, and the factors that affected its performance. Ozer and Royston [8] developed a method based on the Sherman–Morrison matrix inversion formula for determining the optimal parameters for a vibration absorber that is attached to a damped multiple-degrees-of-freedom system. Their method can be used to minimize the motion of selected physical masses or modes of vibration, and to minimize a linear summation of the degrees-of-freedom.

Cha and Pierre [9] developed an approach to passively impose a single node for the normal modes of any arbitrarily supported linear structure by means of attaching a chain of oscillators. Cha [10] generalized the approach to impose multiple nodes for any normal mode of an elastic structure using a set of parallel sprung masses. The focus of Refs. [9,10] was on imposing nodes for the normal modes of a linear structure. Cha [11] used a set of elastically mounted masses to induce a single or multiple nodes anywhere along an elastic structure that is subjected to a harmonically excited localized force, where the nodes are defined as points of zero displacements. Cha [12] extended his previous work by specifying the maximum allowable absorber amplitudes as additional design objectives. An efficient procedure was proposed for choosing the required oscillator parameters, and numerical studies were performed to validate the proposed methodology of imposing nodes at multiple locations along a linear structure during harmonic excitations. In this paper, a set of sprung masses and rotational oscillators are used to enforce one or more fixed nodes, i.e., points of zero displacements and zero slopes, along an arbitrarily supported structure during harmonic excitations. Enforcing fixed nodes is clearly more complicated, because in addition to the zero displacement constraints, the zero slope constraints must also be satisfied. Not surprisingly, enforcing fixed nodes reduces the vibrational level even more compared to imposing nodes only. This is beneficial because it would allow sensitive instruments to be placed near or at fixed nodes where there are little or no vibration. In addition, the proposed scheme allows certain points along the structure to remain stationary without using any rigid supports. Numerical cases studies are presented to verify the utility of the proposed scheme of imposing fixed nodes, and bounds are given for the stiffness parameters of the sprung masses and the rotational oscillators.

2. Theory

2.1. Governing equations

Consider an arbitrarily supported linear structure to which S sprung masses and S rotational oscillators are attached as shown in Fig. 1. A localized harmonic force

$$f(t) = F\mathrm{e}^{\mathrm{j}\omega t} \tag{1}$$

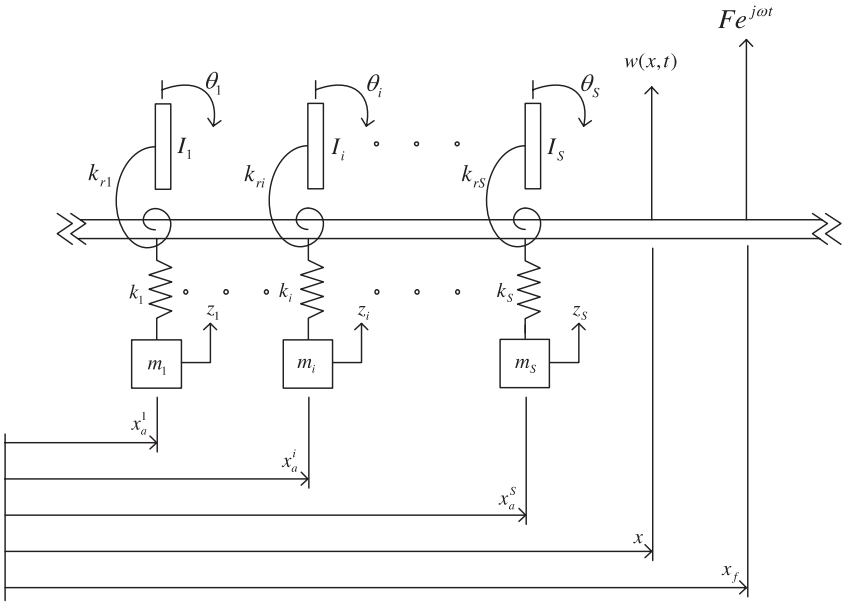

Fig. 1. An arbitrarily supported elastic structure that is subject to a localized harmonic excitation and carrying any number of sprung masses and rotational oscillators.

is applied to the structure at x_f, where F represents the forcing amplitude, ω denotes the driving or excitation frequency, and $j = \sqrt{-1}$. The assumed modes method [13] will be used to formulate the equations of motion. It is a procedure for discretizing an arbitrary structure prior to obtaining the governing equations. This method is utilized instead of other discretization schemes such as the finite element method because it enables one to solve the inverse problem of specifying the sprung mass and rotational oscillator parameters in order to induce fixed nodes anywhere along a linear structure during harmonic excitations.

Using the assumed-modes method, the physical deflection of the structure at any point x is given by

$$w(x,t) = \sum_{i=1}^{N} \phi_i(x)\eta_i(t), \tag{2}$$

where the $\phi_i(x)$ are the eigenfunctions of the linear structure (the elastic structure without any sprung masses) that form the basis functions for this approximate solution, the $\eta_i(t)$ are the corresponding generalized coordinates, and N is the number of modes used in the assumed-modes expansion. The total kinetic and potential energies of the combined system, defined as the linear structure carrying the elastically mounted masses and the rotational oscillators, are given by

$$T = \frac{1}{2}\sum_{i=1}^{N} M_i\dot{\eta}_i^2(t) + \frac{1}{2}\sum_{i=1}^{S}[m_i\dot{z}_i^2(t) + I_i\dot{\theta}_i^2(t)] \tag{3}$$

and

$$V = \frac{1}{2}\sum_{i=1}^{N} K_i\eta_i^2(t) + \frac{1}{2}\sum_{i=1}^{S}[k_i(z_i(t) - w(x_a^i,t))^2 + k_{ri}(\theta_i(t) - w'(x_a^i,t))^2], \tag{4}$$

where M_i and K_i are the respectively, generalized masses and stiffnesses of the linear structure; m_i and k_i are the mass and spring stiffness of the ith oscillator, $z_i(t)$ is its displacement; I_i and k_{ri} are the inertia and rotational spring stiffness for the ith rotational oscillator, $\theta_i(t)$ is its angular displacement; S is the total number of sprung masses/rotational oscillators attached to the linear structure; an overdot denotes a derivative with respect to time t, a prime represents a partial derivative with respect to the spatial coordinate x; x_a^i represents the attachment location of the ith translational and rotational oscillators, and $w(x_a^i,t)$ and

$w'(x_a^i, t)$ represent the lateral displacement and the slope of the beam at x_a^i, respectively. Finally, the generalized force associated with the generalized coordinate $\eta_i(t)$ is

$$F_i(t) = f(t)\phi_i(x_f). \tag{5}$$

Applying Lagrange's equations and assuming simple harmonic motion with the same response frequency as the driving frequency,

$$\eta_i(t) = \bar{\eta}_i e^{j\omega t}, \quad z_i(t) = \bar{z}_i e^{j\omega t}, \quad \theta_i(t) = \bar{\theta}_i e^{j\omega t}, \tag{6}$$

the generalized coordinates $\bar{\boldsymbol{\eta}}$, the amplitudes $\bar{\boldsymbol{z}}$ for the sprung masses and the angular displacements $\bar{\boldsymbol{\theta}}$ for the rotational oscillators for the system of Fig. 1 correspond to the solution of the following matrix equation:

$$\begin{bmatrix} [\mathscr{K}] - \omega^2[\mathscr{M}] & [R_1] & [R_2] \\ [R_1]^T & [k] - \omega^2[m] & [0] \\ [R_2]^T & [0] & [k_r] - \omega^2[I'] \end{bmatrix} \begin{bmatrix} \bar{\boldsymbol{\eta}} \\ \bar{\boldsymbol{z}} \\ \bar{\boldsymbol{\theta}} \end{bmatrix} = \begin{bmatrix} F\boldsymbol{\phi}(x_f) \\ \mathbf{0} \\ \mathbf{0} \end{bmatrix}, \tag{7}$$

where $\bar{\boldsymbol{\eta}} = [\bar{\eta}_1\ \bar{\eta}_2\ \dots\ \bar{\eta}_N]^T$, $\bar{\boldsymbol{z}} = [\bar{z}_1\ \bar{z}_2\ \dots\ \bar{z}_S]^T$, $\bar{\boldsymbol{\theta}} = [\bar{\theta}_1\ \bar{\theta}_2\ \dots\ \bar{\theta}_S]^T$, and the $S \times S$ matrices $[m]$, $[k]$, $[I']$ and $[k_r]$ are all diagonal, whose ith elements are given by m_i, k_i, I_i and k_{ri}, respectively. The $N \times N$ $[\mathscr{M}]$ and $[\mathscr{K}]$ matrices of Eq. (7) are

$$[\mathscr{M}] = [M^d] \quad \text{and} \quad [\mathscr{K}] = [K^d] + \sum_{i=1}^{S} [k_i \boldsymbol{\phi}(x_a^i)\boldsymbol{\phi}^T(x_a^i) + k_{ri}\boldsymbol{\phi}'(x_a^i)\boldsymbol{\phi}'^T(x_a^i)], \tag{8}$$

where $[M^d]$ and $[K^d]$ are diagonal matrices whose ith elements are M_i and K_i; vectors $\boldsymbol{\phi}(x_a^i)$ and $\boldsymbol{\phi}(x_f)$ consist of the eigenfunctions of the linear structure evaluated at x_a^i and x_f, respectively,

$$\boldsymbol{\phi}(x_a^i) = [\phi_1(x_a^i)\ \phi_2(x_a^i)\ \dots\ \phi_N(x_a^i)]^T, \quad \boldsymbol{\phi}(x_f) = [\phi_1(x_f)\ \phi_2(x_f)\ \dots\ \phi_N(x_f)]^T, \tag{9}$$

$\boldsymbol{\phi}'(x_a^i)$ denotes the vector of the derivative of the eigenfunctions evaluated at x_a^i; and the $N \times S$ matrices $[R_1]$ and $[R_2]$ are given by

$$[R_1] = [-k_1\boldsymbol{\phi}(x_a^1)\ \dots\ -k_i\boldsymbol{\phi}(x_a^i)\ \dots\ -k_S\boldsymbol{\phi}(x_a^S)], \tag{10}$$

$$[R_2] = [-k_{r1}\boldsymbol{\phi}'(x_a^1)\ \dots\ -k_{ri}\boldsymbol{\phi}'(x_a^i)\ \dots\ -k_{rS}\boldsymbol{\phi}'(x_a^S)]. \tag{11}$$

To induce fixed nodes at any desired locations, x_n^r, along the linear structure requires that the displacements and slopes of the linear structure at x_n^r be zero simultaneously, i.e.,

$$w(x_n^r, t) = \sum_{i=1}^{N} \phi_i(x_n^r)\eta_i(t) = \boldsymbol{\phi}^T(x_n^r)\boldsymbol{\eta} = \boldsymbol{\phi}^T(x_n^r)\bar{\boldsymbol{\eta}}e^{j\omega t} = 0, \quad r = 1, \dots, S, \tag{12}$$

$$w'(x_n^r, t) = \sum_{i=1}^{N} \phi_i'(x_n^r)\eta_i(t) = \boldsymbol{\phi}'^T(x_n^r)\boldsymbol{\eta} = \boldsymbol{\phi}'^T(x_n^r)\bar{\boldsymbol{\eta}}e^{j\omega t} = 0, \quad r = 1, \dots, S. \tag{13}$$

Once the linear structure and its boundary conditions are specified, the attachment locations x_a^i are given, and the excitation frequency ω and the excitation location x_f are known, Eqs. (7), (12) and (13) can be used together to solve for the required sprung mass parameters, m_i and k_i, and the required rotational oscillator parameters, I_i and k_{ri}, in order to impose fixed nodes at x_n^r.

2.2. Oscillators and node locations are collocated

When the attachment and the fixed node locations coincide, or otherwise known as *collocated*, determining the required sprung mass and rotational oscillator parameters to induce fixed nodes is trivial. From Eq. (7), note that if

$$k_i = m_i\omega^2 \quad \text{and} \quad k_{ri} = I_i\omega^2, \quad i = 1, \dots, S, \tag{14}$$

then

$$[R_1]^{\mathrm{T}}\bar{\boldsymbol{\eta}} = \mathbf{0} \quad \text{and} \quad [R_2]^{\mathrm{T}}\bar{\boldsymbol{\eta}} = \mathbf{0}. \tag{15}$$

Because the attachment and the fixed node locations are collocated, $x_a^i = x_n^i$, in which case the ith row of both expressions in Eq. (15) yield

$$-k_i\boldsymbol{\phi}^{\mathrm{T}}(x_a^i)\bar{\boldsymbol{\eta}} = -k_i\boldsymbol{\phi}^{\mathrm{T}}(x_n^i)\bar{\boldsymbol{\eta}} = 0, \quad i = 1,\ldots,S, \tag{16}$$

$$-k_{ri}\boldsymbol{\phi}'^{\mathrm{T}}(x_a^i)\bar{\boldsymbol{\eta}} = -k_{ri}\boldsymbol{\phi}'^{\mathrm{T}}(x_n^i)\bar{\boldsymbol{\eta}} = 0, \quad i = 1,\ldots,S, \tag{17}$$

which clearly satisfy Eqs. (12) and (13). For a given excitation frequency, as long as the sprung mass and rotational oscillator parameters satisfy Eq. (14), fixed nodes will be induced at the attachment locations. Finally, the selection of the sprung mass and rotational oscillator parameters is certainly not unique. The eventual choice is governed by the tolerable vibration amplitudes of the sprung masses and the tolerable angular displacements of the rotational oscillators.

2.3. Oscillators and node locations are not collocated

Consider an elastic structure subjected to a localized harmonic input. For a certain application, a fixed node or multiple fixed nodes are desired along the linear structure for a given excitation frequency. However, due to various physical constraints, the sprung masses and the rotational oscillators cannot be attached at the desired node locations, but instead at some other points along the linear structure. For this case, the attachment and the fixed node locations are said to be *non-collocated*. When the attachment and the fixed node locations are non-collocated, Eq. (7), of size $(N+2S)\times(N+2S)$, can be reduced by simple algebraic manipulation. Using Eq. (7), the $\bar{z}_i$ and $\bar{\theta}_i$ are found to be

$$\bar{z}_i = \frac{k_i\boldsymbol{\phi}^{\mathrm{T}}(x_a^i)}{k_i - \omega^2 m_i}\bar{\boldsymbol{\eta}}, \quad i = 1,\ldots,S, \tag{18}$$

$$\bar{\theta}_i = \frac{k_{ri}\boldsymbol{\phi}'^{\mathrm{T}}(x_a^i)}{k_{ri} - \omega^2 I_i}\bar{\boldsymbol{\eta}}, \quad i = 1,\ldots,S. \tag{19}$$

Substituting Eqs. (18) and (19) into Eq. (7), the following matrix equation, of size $N\times N$, is obtained:

$$\left\{[K^d] + \sum_{i=1}^{S}[\sigma_i\boldsymbol{\phi}(x_a^i)\boldsymbol{\phi}^{\mathrm{T}}(x_a^i) + \tau_i\boldsymbol{\phi}'(x_a^i)\boldsymbol{\phi}'^{\mathrm{T}}(x_a^i)] - \omega^2[M^d]\right\}\bar{\boldsymbol{\eta}} = F\boldsymbol{\phi}(x_f), \tag{20}$$

where

$$\sigma_i = \frac{k_i m_i\omega^2}{m_i\omega^2 - k_i} \quad \text{and} \quad \tau_i = \frac{k_{ri}I_i\omega^2}{I_i\omega^2 - k_{ri}}. \tag{21}$$

Incidentally, once the m_i, k_i, I_i, k_{ri} and x_a^i have been selected, the natural frequencies of the modified structure, i.e., the structure carrying the translational and rotational oscillators, may be found from the zeros of the characteristic determinant of the coefficient matrix of $\bar{\boldsymbol{\eta}}$ of Eq. (20). Assuming that the excitation frequency does not coincide with any natural frequencies of the modified system, the coefficient matrix of Eq. (20) can be inverted to give

$$\bar{\boldsymbol{\eta}} = \left\{[K^d] + \sum_{i=1}^{S}[\sigma_i\boldsymbol{\phi}(x_a^i)\boldsymbol{\phi}^{\mathrm{T}}(x_a^i) + \tau_i\boldsymbol{\phi}'(x_a^i)\boldsymbol{\phi}'^{\mathrm{T}}(x_a^i)] - \omega^2[M^d]\right\}^{-1} F\boldsymbol{\phi}(x_f), \tag{22}$$

which allows Eqs. (12) and (13), the constraint equations that dictate the fixed node locations, to be rewritten as

$$\boldsymbol{\phi}^{\mathrm{T}}(x_n^r)\left\{[K^d] + \sum_{i=1}^{S}[\sigma_i\boldsymbol{\phi}(x_a^i)\boldsymbol{\phi}^{\mathrm{T}}(x_a^i) + \tau_i\boldsymbol{\phi}'(x_a^i)\boldsymbol{\phi}'^{\mathrm{T}}(x_a^i)] - \omega^2[M^d]\right\}^{-1} F\boldsymbol{\phi}(x_f) = 0, \quad r = 1,\ldots,S, \tag{23}$$

$$\boldsymbol{\phi}'^{\mathrm{T}}(x_n^r)\left\{[K^d]+\sum_{i=1}^{S}\sigma_i\boldsymbol{\phi}(x_a^i)\boldsymbol{\phi}^{\mathrm{T}}(x_a^i)+\tau_i\boldsymbol{\phi}'(x_a^i)\boldsymbol{\phi}'^{\mathrm{T}}(x_a^i)]-\omega^2[M^d]\right\}^{-1}F\boldsymbol{\phi}(x_f)=0,\quad r=1,\ldots,S. \tag{24}$$

Eqs. (23) and (24) can be used to solve for the required sprung mass and rotational oscillator parameters in order to induce a single or multiple fixed nodes at x_n^r.

Eqs. (23) and (24) yield a set of $2S$ equations. By assuming the excitation frequency ω, the attachment locations x_a^i, and the excitation location x_f, all are specified, these $2S$ equations lead to a set of non-linear algebraic equations in terms of σ_i and τ_i, which can be solved simultaneously so that the specified x_n^r are fixed nodes. Because the $2S$ equations are generally totally independent, the solution to these simultaneous non-linear algebraic equations can be difficult if not impossible to obtain analytically. In this paper, the MATLAB routine fsolve is employed to obtain the solution of a system of non-linear algebraic equations numerically using a quasi-Newton method. To execute fsolve, a set of initial guesses must be provided for the unknowns. For these initial guesses, if fsolve does not converge to a solution, then fsolve is executed again with a different set of starting values until a solution is obtained.

Because the $2S$ equations are highly non-linear, determining the solution to these equations may be computationally taxing using fsolve. To expedite convergence, an iterative method is proposed that quickly leads to a set of desired solution. The proposed iterative scheme is based on varying the number of modes used in the assumed modes method. First let the number of assumed modes N be small and use different sets of initial guesses to determine the solution to these equations. Because N is relatively small, this step can be completed very quickly. Once the optimal initial guesses are determined, use the solution given by fsolve under the optimal initial guesses as the input for the next iteration, and let N be a larger number. The iteration process is repeated until N becomes sufficiently large, and the output of fsolve converges to a set of theoretically feasible solution.

Incidentally, Cha [11,12] imposed nodes or points of zero displacements using properly tuned sprung masses, and found that using the assumed modes method with $N = 15$ was sufficient to converge to a set of solution. In this paper, fixed nodes are induced, where points of zero displacements and zero slopes are enforced. Interestingly, with the additional constraints of zero slopes, the solution is found to converge very slowly, and substantially more modes are required in the assumed modes method to ensure accurate results. In particular, when the attachment and the fixed node locations are not collocated, the number of modes used in the assumed modes method can be as large as 1000 to ensure sufficient accuracy.

The proposed technique of solving for the σ_i and τ_i in order to impose fixed nodes at x_n^r is very robust. In all of the cases considered, the iteration process successfully converged to a set of theoretically feasible solutions. Finally, if there is no set of σ_i and τ_i that satisfies the $2S$ non-linear algebraic equations, then one can change one or more of the attachment locations, x_a^i, to obtain the required σ_i and τ_i so that fixed nodes at x_n^i can be induced for the given x_f and ω.

Once the required σ_i and τ_i have been obtained numerically, the corresponding sprung mass and rotational oscillator parameters can be readily determined. Assume the stiffnesses, k_i and k_{ri}, are specified, then from Eq. (21), the required masses and inertias are

$$m_i=\frac{k_i\sigma_i}{(\sigma_i-k_i)\omega^2}\quad\text{and}\quad I_i=\frac{k_{ri}\tau_i}{(\tau_i-k_{ri})\omega^2}. \tag{25}$$

While σ_i and τ_i can be either positive or negative, to be physically meaningful, all of the physical parameters, m_i, k_i, I_i and k_{ri}, must be strictly positive. Thus, Eq. (25) gives the bounds on the stiffnesses, i.e.,

$$\text{if } \sigma_i>0\Longrightarrow 0<k_i<\sigma_i\quad \text{if } \sigma_i<0\Longrightarrow k_i>0, \tag{26}$$

$$\text{if } \tau_i>0\Longrightarrow 0<k_{ri}<\tau_i\quad \text{if } \tau_i<0\Longrightarrow k_{ri}>0. \tag{27}$$

These bounds serve as the design guide for selecting the stiffnesses of the sprung masses and the rotational oscillators. Finally, the selection of the oscillator parameters is not unique. For a given set of σ_i and τ_i, infinite combinations of (k_i, m_i) and (k_{ri}, I_i) are theoretically feasible. The actual choice is governed by the tolerable amplitudes of the oscillator masses and inertias.

3. Results

Because the assumed-modes method was used to formulate the equations of motion, the proposed procedures can be easily implemented to impose a single or multiple fixed nodes for any arbitrarily supported linear structure during harmonic excitations. Without any loss of generality, a simply supported uniform Euler–Bernoulli beam will be considered, whose normalized (with respect to the mass per unit length, ρ, of the beam) eigenfunctions are given by

$$\phi_i(x) = \sqrt{\frac{2}{\rho L}} \sin\left(\frac{i\pi x}{L}\right), \tag{28}$$

such that the generalized masses and stiffnesses of the beam become $M_i = 1$ and $K_i = (i\pi)^4 EI/(\rho L^4)$, respectively, where E is the Young's modulus, I is the moment of inertia of the cross-section of the beam.

Eqs. (23) and (24) will be used to find the σ_i and τ_i in order to impose one or more fixed nodes at x_n^r. To validate the results of the assumed modes method and the σ_i and τ_i of Eqs. (23) and (24), a finite element model of the beam carrying sprung masses and rotational oscillators is constructed, where the stiffnesses of the oscillators are specified based on available translational and rotational springs, and the masses and inertias of the oscillators are given by the solutions of Eq. (25). The finite element model will also be subjected to the same localized input. In all of the subsequent examples, the steady state deformed shape of the beam, the natural frequencies of the structure carrying the properly tuned translational and rotational oscillators, and the mass amplitudes and inertia angular displacements will be determined by using both the assumed modes and the finite element methods. In using the latter approach, the beam is discretized into 100 finite elements of equal length. Cha [11,12] used properly tuned spring–mass systems to effectively impose points of zero displacements or nodes anywhere along a linear structure during harmonic excitations. To illustrate the benefits of imposing zero slope constraints in addition to the zero displacement constraints, the beam deformations will also be compared with those where only spring–mass systems are attached. In all of the subsequent numerical examples, $N = 15$ when one or more nodes (points of zero displacements) are induced, for both the collocated and non-collocated cases; $N = 500$ when one or more fixed nodes (points of zero displacements and zero slopes) are imposed for the collocated cases and $N = 1000$ for the non-collocated cases. These values of N are chosen for consistency and to guarantee that the results (including the deformed shape of the beam, its natural frequencies and oscillator amplitudes) match those obtained by using the finite element method.

3.1. Collocated

For a given application, it is wished that a fixed node be imposed at $x_n = 0.31L$, for a concentrated harmonic force of amplitude F, an excitation frequency of $\omega = 21\sqrt{EI/(\rho L^4)}$, and an excitation location of $x_f = 0.77L$. The steady state lateral displacement of the beam is shown in Fig. 2. The dashed line corresponds to the deformed shape of the beam with no oscillator, and the horizontal line represents the configuration of the undeformed beam. The dash–dotted line shows the deformed shape of the beam with a spring–mass system attached at $x_a = 0.31L$, whose parameters are chosen such that $k = m\omega^2$. Note that a node is induced at the desired location of $0.31L$ [11]. The solid line gives the deformed shape of the beam with both a sprung mass and a rotational oscillator attached at $x_a = 0.31L$, where $k = m\omega^2$ and $k_r = I_r\omega^2$. Note that by attaching a tuned rotational oscillator in addition to a tuned spring–mass system, the attachment location not only remains stationary but also has zero slope. More importantly, the steady state response of the beam carrying properly tuned translational and rotational oscillators is substantially suppressed compared to the beam carrying a spring–mass attachment only, and the vibration of the beam between 0 and $0.35L$ is completely quenched. Physically, the translational and rotational oscillators exert a force and moment equal in magnitude and opposite in direction to the equivalent disturbance force and moment that act at x_n, thus causing x_n to undergo zero displacement and zero slope. Finally, note that attaching a properly tuned spring–mass system to enforce a node is analogous to adding a simply supported constraint at the node location (see the dash–dotted

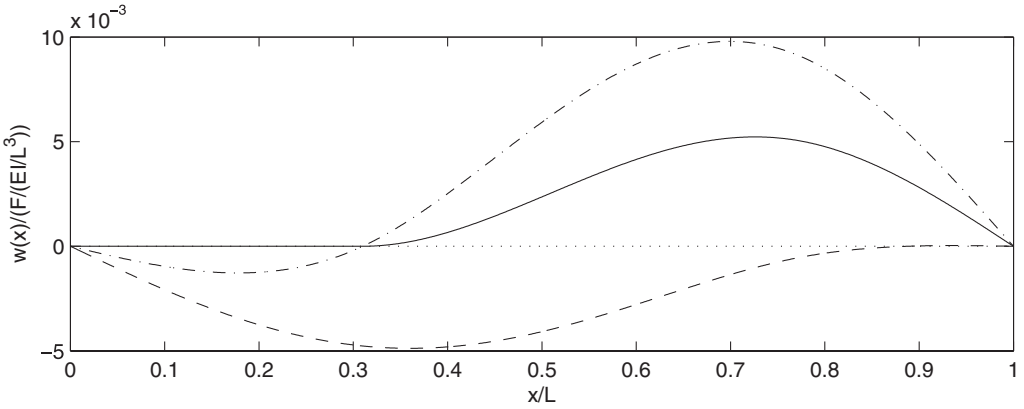

Fig. 2. The steady state deformed shapes of a uniform simply supported Euler–Bernoulli beam with a sprung mass as well as a rotational oscillator (solid line), with a sprung mass only (dash–dotted line), and without any oscillator (dashed line). The horizontal line represents the configuration of the undeformed beam. The system parameters are $\omega = 21\sqrt{EI/(\rho L^4)}$, $x_f = 0.77L$ and $x_a = 0.31L$. The attachment and node locations are collocated.

Table 1
The first six natural frequencies of a uniform simply supported Euler–Bernoulli beam carrying one sprung mass and one rotational oscillator attached at $x_a = 0.31L$

Natural frequency	Assumed modes ($N = 500$)	Finite element ($N = 100$)
ω_1	0.97615E+01	0.97615E+01
ω_2	0.20559E+02	0.20555E+02
ω_3	0.21059E+02	0.21059E+02
ω_4	0.39684E+02	0.39684E+02
ω_5	0.89800E+02	0.89800E+02
ω_6	1.58450E+02	1.58450E+02

The system parameters are $k = 1.0EI/L^3$, $m = 2.26757 \times 10^{-3}\rho L$, $k_r = 1.0EI/L$ and $I_r = 2.26757 \times 10^{-3}\rho L^3$. The natural frequencies are non-dimensionalized by dividing by $\sqrt{EI/(\rho L^4)}$.

Table 2
Vibration amplitudes of the translational and rotational oscillators, obtained using the assumed modes and the finite element methods

	Assumed modes	Finite element
z	9.98141E−01	1.00008E+00
θ	1.94571E−01	1.94208E−01

The system parameters are identical to those of Fig. 2. The stiffnesses are $k = 1.0EI/L^3$ and $k_r = 1.0EI/L$. The displacement z of the oscillator mass is non-dimensionalized by dividing by L.

line). Similarly, attaching a properly tuned spring–mass system and a properly tuned rotational oscillator to enforce a fixed node is analogous to adding a fixed support constraint at the node location (see the solid line).

To validate the previous results, a finite element model of the beam carrying a translational and rotational oscillators at $x_a = 0.31L$, whose parameters satisfy $k = m\omega^2$ and $k_r = I_r\omega^2$, is developed. The steady state deformed shape of the finite element beam model is identical to that shown in Fig. 2, and it will not be shown. In Table 1 are given the natural frequencies of the combined system (the beam carrying the two oscillators), obtained by using the assumed modes (with $N = 500$) and the finite element method (where the beam is discretized into 100 elements of equal length). Note the excellent agreement between the two approaches. Table 2 shows the mass and inertia amplitudes when the beam is subjected to the given harmonic excitation,

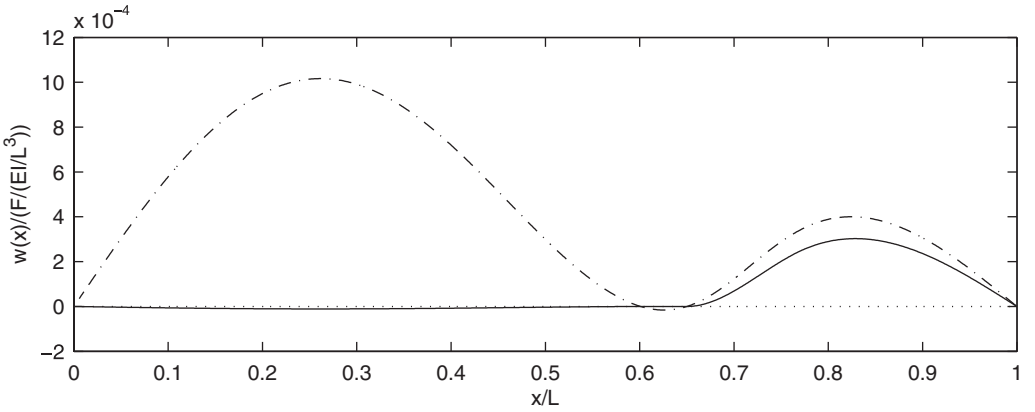

Fig. 3. The steady state deformed shapes of a uniform simply supported Euler–Bernoulli beam with a sprung mass as well as a rotational oscillator (solid line), and with a sprung mass only (dash–dotted line). The horizontal line represents the configuration of the undeformed beam. The system parameters are $\omega = 39.5\sqrt{EI/(\rho L^4)}$, $x_f = 0.77L$ and $x_a = 0.65L$. The attachment and node locations are collocated.

where $k = 1.0EI/L^3$ and $k_r = 1.0EI/L$. Note again how well the assumed modes and the finite element results track one another. Incidentally, in all of the subsequent examples, the assumed modes and the finite element results agree very well. Thus, unless otherwise stated, the deformed shape, natural frequencies and mass/inertia amplitudes obtained by using the finite element method will not be shown for the sake of brevity.

Consider now a simply supported beam subjected to a concentrated harmonic excitation with a frequency of $\omega = 39.5\sqrt{EI/(\rho L^4)}$, which nearly coincides with the second natural frequency of a simply supported beam with no attachment, given by $4\pi^2\sqrt{EI/(\rho L^4)}$. The system parameters are $x_f = 0.77L$ and $x_a = 0.65L$. For an arbitrarily chosen set of k and k_r, the mass and inertia are determined by $m = k/\omega^2$ and $I_r = k_r/\omega^2$ so that the attachment location becomes a fixed node. In Fig. 3 is shown the deformed shape of the beam, where the solid line corresponds to the response shape of the beam carrying a translational and a rotational oscillator, and the dash–dotted line corresponds to the deformed shape of the beam with one sprung mass. The deformed shape for a simply supported beam with no attachment is not illustrated, because its amplitude is orders of magnitude larger due to resonance. When the beam is carrying a properly tuned sprung mass only, a node is induced at $0.65L$; when the beam is carrying tuned translational and rotation oscillators, the vibration in the region between 0 and $0.67L$ along the beam is substantially suppressed compared to the beam with a single sprung mass attachment. Moreover, note that when a fixed node is induced, the deformation at any point along the beam is less than that of the beam where a node is imposed.

Consider a different application where two fixed nodes are desired, at $x_n^1 = 0.2L$ and $x_n^2 = 0.7L$, for $\omega = 57\sqrt{EI/(\rho L^4)}$ and $x_f = 0.87L$. In Fig. 4 is shown the steady state lateral displacement of the beam with and without attachments. For the beam carrying sprung masses, the oscillator parameters satisfy $k_i = m_i\omega^2$; for the beam carrying translational and rotational oscillators, the oscillator parameters are tuned according to $k_i = m_i\omega^2$ and $k_{ri} = I_i\omega^2$. While the deformed shape of the beam with only sprung masses (see the dash–dotted line) has nodes at $0.2L$ and $0.7L$ as expected, the response of the beam with both translational and rotational oscillators (see the solid line) is completely suppressed in the region between 0 and $0.7L$. Thus, by attaching translational and rotational oscillators at the appropriate locations, one can quench the vibration more effectively than attaching sprung masses only. Moreover, note that the vibrational amplitude at every point is smaller for the beam with fixed nodes.

Table 3 lists the mass and inertia amplitudes of the translational and rotational oscillators of Fig. 4 for different sets of k_i and k_{ri} values. For simplicity, $k_1 = k_2$ and $k_{r1} = k_{r2}$ since in application, using the same springs would be the most convenient. Although these stiffnesses do not affect the steady state deformation of

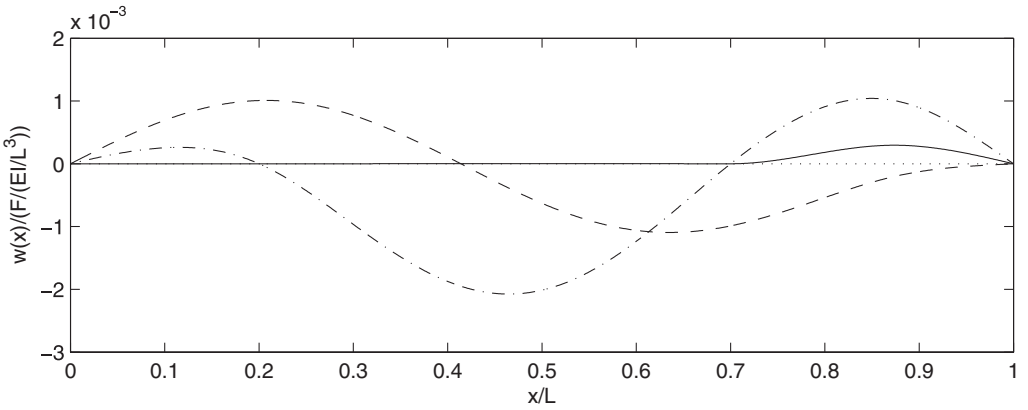

Fig. 4. The steady state deformed shapes of a uniform simply supported Euler–Bernoulli beam with two sprung masses as well as two rotational oscillators (solid line), with two sprung masses only (dash–dotted line), and without any oscillator (dashed line). The system parameters are $\omega = 57\sqrt{EI/(\rho L^4)}$, $x_f = 0.87L$, $x_a^1 = 0.2L$ and $x_a^2 = 0.7L$. The attachment and node locations are collocated.

Table 3
The vibration amplitudes for the sprung masses and the rotational oscillators for different stiffnesses

k_1, k_2	k_{r1}, k_{r2}	m_1, m_2	I_1, I_2	z_1	z_2	θ_1	θ_2
2	2	6.1557E−04	6.1557E−04	4.2237E−04	3.5235E−01	5.5331E−05	3.0095E−02
10	15	3.0779E−03	4.6168E−03	8.4474E−05	7.0469E−02	7.3775E−06	4.0126E−03
25	20	7.6947E−03	6.1557E−03	3.3790E−05	2.8188E−02	5.5331E−06	3.0095E−03
40	30	1.2311E−02	9.2336E−03	2.1119E−05	1.7617E−02	3.6887E−06	2.0063E−03
80	50	2.4623E−02	1.5389E−02	1.0559E−05	8.8087E−03	2.2131E−06	1.2038E−03

The corresponding mass and inertia parameters are also shown. The system parameters are $\omega = 57\sqrt{EI/(\rho L^4)}$, $x_f = 0.87L$, $x_a^1 = 0.2L$ and $x_a^2 = 0.7L$. The attachment and node locations are collocated. The stiffnesses k_i and k_{ri} of the springs are non-dimensionalized by dividing by EI/L^3 and EI/L, respectively. The masses m_i and inertias I_i are non-dimensionalized by dividing by ρL and ρL^3, respectively. The displacements z_1 and z_2 of the oscillator masses are non-dimensionalized by dividing by L.

the beam, they dictate the vibration amplitudes of the oscillators. By varying k_i and k_{ri} and by setting $m_i = k_i/\omega^2$ and $I_i = k_{ri}/\omega^2$, different amplitudes can be obtained. Moreover, each k_i or k_{ri} can be tuned independently to determine the vibration amplitude of the corresponding oscillator without influencing the vibration of the other oscillator. In Table 3, note that by increasing k_i or k_{ri}, the vibration amplitude of the corresponding oscillator decreases. This suggests that by choosing sufficiently large k_i or k_{ri}, small vibration amplitude for each oscillator can be obtained. However, increasing k_i or k_{ri} increases the mass or inertia since $m_i = k_i/\omega^2$ and $I_i = k_{ri}/\omega^2$. Thus, the optimal value of k_i or k_{ri} of each oscillator should be selected carefully according to the practical application. In addition, for each translational oscillator, the product of its mass and vibration amplitude remains constant regardless of what stiffness k_i is chosen; the same results were obtained when only nodes are imposed [12]. In particular, $m_1 z_1 = 2.6000\text{E}-07 F\rho L^4/(EI)$ and $m_2 z_2 = 2.1690\text{E}-04 F\rho L^4/(EI)$ for the system parameters of Fig. 4. Numerically, the product of $I_i\theta_i$ for each rotational oscillator is also found to remain unchanged. Specifically, $I_1\theta_1 = 3.4060\text{E}-08 F\rho L^5/(EI)$ and $I_2\theta_2 = 1.8526\text{E}-05 F\rho L^5/(EI)$. The aforementioned results have important practical implications, since once the product of $m_i z_i$ and $I_i\theta_i$ are known explicitly, the oscillator parameters can be easily tuned to satisfy the maximum tolerable amplitudes for the mass and inertia of the translational and rotational oscillators, respectively.

As noted in Ref. [11], a region of zero displacement can be extended by adding more sprung masses to induce more nodes. Interestingly, the same or better results can often be achieved with fewer fixed nodes. In

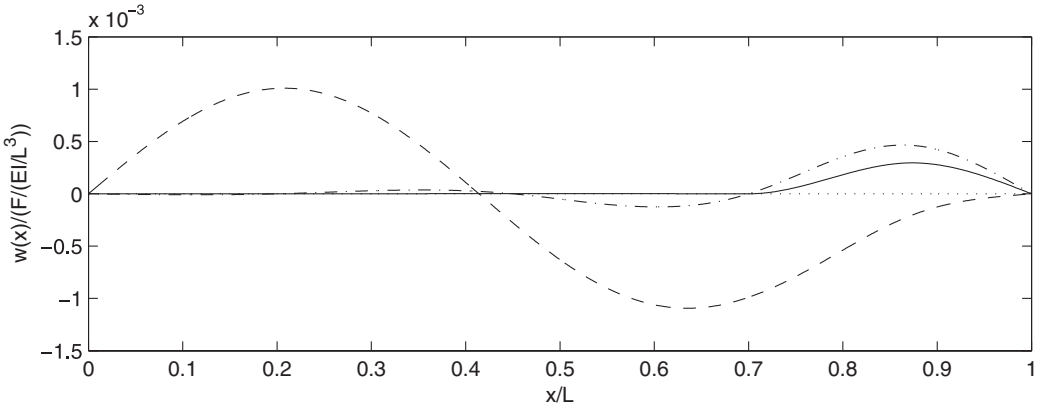

Fig. 5. The steady state deformed shapes of a uniform simply supported Euler–Bernoulli beam with two sprung masses as well as two rotational oscillators at $0.2L$ and $0.7L$ (solid line), with three sprung masses only at $0.2L$, $0.45L$ and $0.7L$ (dash–dotted line), and without any oscillator (dashed line). The system parameters are $\omega = 57\sqrt{EI/(\rho L^4)}$ and $x_f = 0.87L$. The attachment and node locations are collocated.

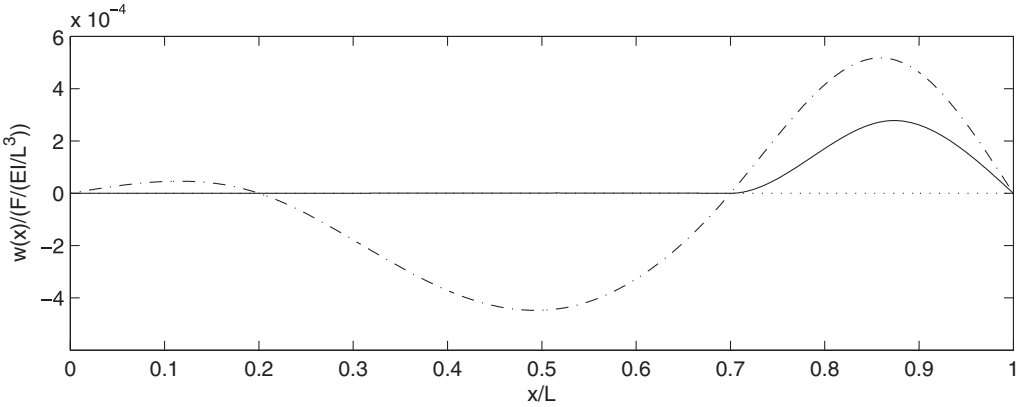

Fig. 6. The steady state deformed shapes of a uniform simply supported Euler–Bernoulli beam with two sprung masses as well as two rotational oscillators (solid line), with two sprung masses only (dash–dotted line), and without any oscillator (dashed line). The system parameters are $\omega = 39.5\sqrt{EI/(\rho L^4)}$, $x_f = 0.87L$, $x_a^1 = 0.2L$ and $x_a^2 = 0.7L$. The attachment and node locations are collocated.

Fig. 5 is shown the deformed shape of a simply supported beam under the same harmonic excitation as that of Fig. 4, except now a third node is desired at $0.45L$. Thus, an additional sprung mass is attached at the new node location, and the vibration of the beam in the region between 0 and $0.7L$ is greatly quenched compared to the beam of Fig. 4 when only two nodes are specified. However, the vibration of the beam between 0 and $0.7L$ when only two fixed nodes are imposed at $0.2L$ and $0.7L$ (the solid line) is still much lower than the vibration of the beam where three nodes are enforced at $0.2L$, $0.45L$ and $0.7L$ (the dash–dotted line). Therefore, attaching translational and rotational oscillators to enforce the zero displacement and zero slope constraints is often a more efficient way to quench vibration in a beam than by attaching sprung masses only to enforce the zero displacement constraints. This is clearly beneficial because for structures where the attachment locations are limited due to physical access, one can use fewer attachment points to suppress the vibration of the beam.

Consider again the system of Fig. 4, except now the excitation frequency is at $39.5\sqrt{EI/(\rho L^4)}$, which nearly coincides with the second natural frequency of a simply supported beam with no attachment. In Fig. 6 is shown the deformed shape of the beam, where the solid and dash–dotted correspond to the deformed shape of the beam carrying translational/rotational oscillators and carrying sprung masses only, respectively. The

deformed shape of the bare beam, i.e., the beam without any attachment, is not illustrated because the excitation frequency is near resonance. When two tuned sprung masses are attached to the beam, nodes are induced at $0.2L$ and $0.7L$. When two sets of translational and rotational oscillators are attached to the beam, not only are fixed nodes enforced at the desired locations, but the beam remains nearly stationary in the region between 0 and $0.7L$, even though the beam is being excited with a frequency that is near the bare beam's second natural frequency. This example clearly illustrates the effectiveness of using properly tuned translational and rotational oscillators to induce fixed nodes and to suppress vibration.

3.2. Non-collocated

Consider now cases where the attachment and node locations are not collocated. In Fig. 7 is shown the steady state lateral displacement of a simply supported beam with a concentrated harmonic force applied at $x_f = 0.77L$, with a forcing frequency of $\omega = 57\sqrt{EI/(\rho L^4)}$ and with the desired fixed node location at $x_n = 0.31L$. However, the oscillators are placed at $x_a = 0.65L$ because of space constraint. In this case, Eqs. (23) and (24) can be used to obtain the σ and τ required to induce a fixed node. Solving Eqs. (23) and (24) simultaneously yields $\sigma = 1.35628 \times 10^6 EI/L^3$ and $\tau = 5.49823 \times 10^3 EI/L$ when $N = 1000$ is used. For the given σ and τ, the deformed shape of the beam is unique. Therefore, there exists an infinite number of (k, m) and (k_r, I_r) combinations that can be used to induce fixed nodes theoretically, and the oscillator parameters should be chosen according to the maximum tolerable oscillator amplitudes [12]. By using the approach outlined in Ref. [11] to induce a node with zero displacement only, one finds $\sigma = 1.89511 \times 10^3 EI/L^3$ for $N = 15$. In Fig. 7, the deformed shapes for a bare beam, for a beam with a properly tuned spring–mass system, and for a beam carrying a tuned sprung mass/rotational oscillator are given by the dashed, dash–dotted, and solid lines, respectively. Note that the beam carrying a properly tuned sprung mass has a node at the desired location of $0.31L$, and that the vibration is substantially suppressed from 0 to $0.31L$ compared to the response of the bare beam. Attaching a tuned translational and a rotational oscillator to the beam, on the other hand, reduces the vibration even more. Note that not only is fixed node induced at $0.31L$, but the beam remains nearly motionless in the region between 0 and $0.65L$. Moreover, its response is drastically quenched compared to the deformed shape of the beam carrying only an elastically mounted mass.

In Fig. 8 is shown the deformed shape of the beam under harmonic excitation, with the same ω and x_f as those of Fig. 7, except now the oscillators are moved from $x_a = 0.65L$ to $0.72L$. The desired fixed node is still located at $x_n = 0.31L$. Eqs. (23) and (24) give $\sigma = 2.83999 \times 10^6 EI/L^3$ and $\tau = 6.71438 \times 10^3 EI/L$. To impose a node with only a spring–mass system [11], one finds $\sigma = 3.92203 \times 10^3 EI/L^3$. In Fig. 8, note that by

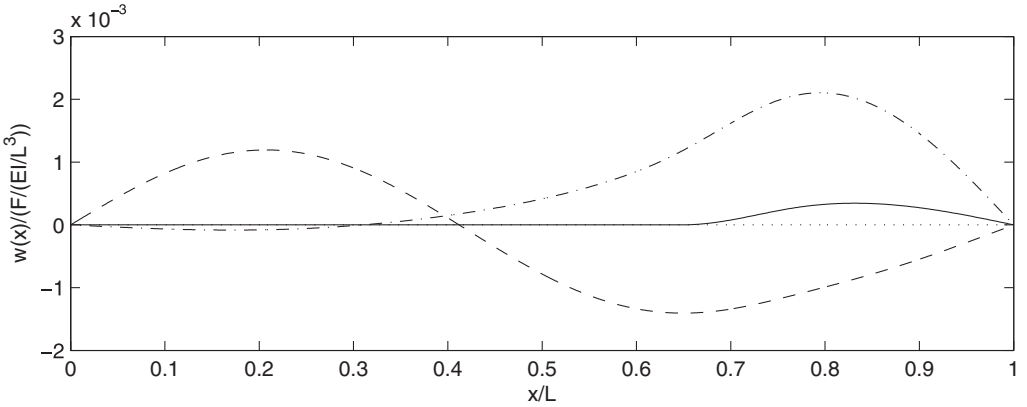

Fig. 7. The steady state deformed shapes of a uniform simply supported Euler–Bernoulli beam with a sprung mass as well as a rotational oscillator (solid line), with a sprung mass only (dash–dotted line), and without any oscillator (dashed line). The system parameters for the solid line are $\omega = 57\sqrt{EI/(\rho L^4)}$, $x_f = 0.77L$, $x_a = 0.65L$, $x_n = 0.31L$, $\sigma = 1.35628 \times 10^6 EI/L^3$ and $\tau = 5.49823 \times 10^3 EI/L$. For the dash–dotted line, $\sigma = 1.89511 \times 10^3 EI/L^3$. The attachment and node locations are not collocated.

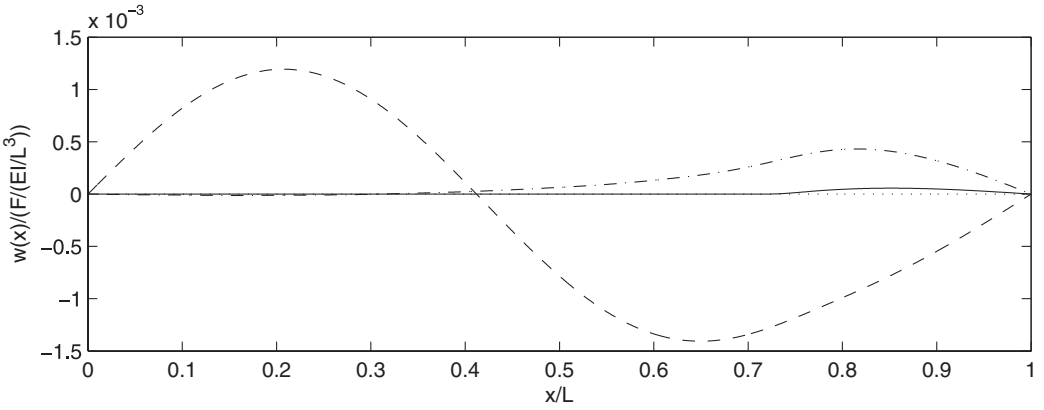

Fig. 8. The steady state deformed shapes of a uniform simply supported Euler–Bernoulli beam with a sprung mass as well as a rotational oscillator (solid line), with a sprung mass only (dash–dotted line), and without any oscillator (dashed line). The system parameters for the solid line are $\omega = 57\sqrt{EI/(\rho L^4)}$, $x_f = 0.77L$, $x_a = 0.72L$, $x_n = 0.31L$, $\sigma = 2.83999 \times 10^6 EI/L^3$ and $\tau = 6.71438 \times 10^3 EI/L$. For the dash–dotted line, $\sigma = 3.92203 \times 10^3 EI/L^3$. The attachment and node locations are not collocated.

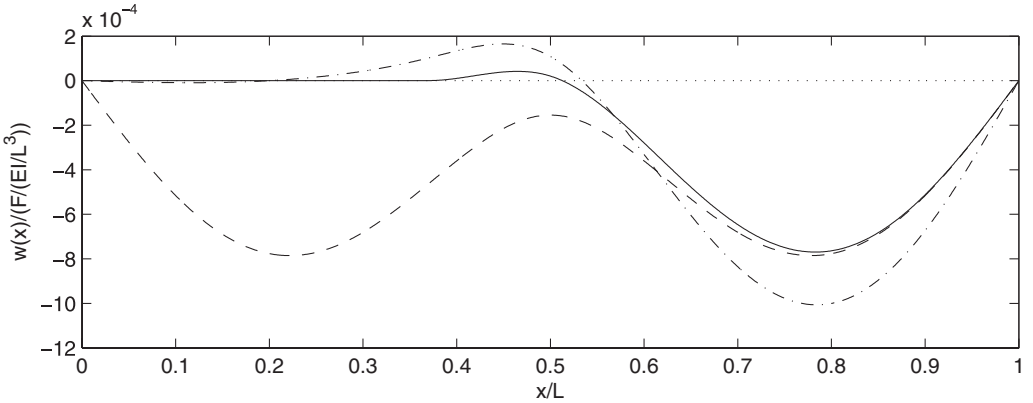

Fig. 9. The steady state deformed shapes of a uniform simply supported Euler–Bernoulli beam with a sprung mass as well as a rotational oscillator (solid line), with a sprung mass only (dash–dotted line), and without any oscillator (dashed line). The system parameters for the solid line are $\omega = 57\sqrt{EI/(\rho L^4)}$, $x_f = 0.5L$, $x_a = 0.37L$, $x_n = 0.2L$, $\sigma = 1.34184 \times 10^6 EI/L^3$ and $\tau = 7.40964 \times 10^3 EI/L$. For the dash–dotted line, $\sigma = 5.55693 \times 10^3 EI/L^3$. The attachment and node locations are not collocated.

simply changing the attachment location, the vibrational levels for both the beam with nodes and the beam with fixed nodes are substantially reduced compared to the results of Fig. 7. Additionally, note that the beam carrying the translational and rotational oscillators becomes nearly stationary after the attachment location has been changed. The dramatic reduction in the vibration of the beam implies that by properly selecting the attachment location, one can suppress the vibration even more effectively. Thus, the attachment locations can also be used as design parameters. By attaching tuned oscillators at optimal locations, one can extend the region along the beam where the vibration is minimized.

In engineering applications, the excitation force is often applied at the midspan of the beam. Fig. 9 is an illustration of the deformation of the beam for this particular case, where $x_f = 0.5L$, $\omega = 57\sqrt{EI/(\rho L^4)}$, $x_a = 0.37L$ and $x_n = 0.2L$. Solving Eqs. (23) and (24) one obtains $\sigma = 1.34184 \times 10^6 EI/L^3$ and $\tau = 7.40964 \times 10^3 EI/L$. To impose a node with only a spring–mass system [11], one finds $\sigma = 5.55693 \times 10^3 EI/L^3$. Note that by attaching properly tuned translational and rotational oscillators, the point at $0.2L$ becomes a fixed node,

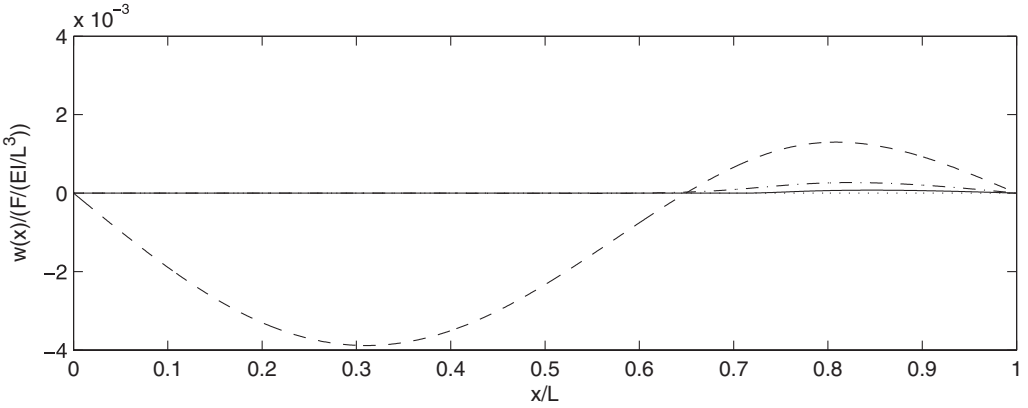

Fig. 10. The steady state deformed shapes of a uniform simply supported Euler–Bernoulli beam with two sprung masses as well as two rotational oscillators (solid line), with two sprung masses only (dash–dotted line), and without any oscillator (dashed line). The system parameters for solid line are $\omega = 27\sqrt{EI/(\rho L^4)}$, $x_f = 0.77L$, $x_a^1 = 0.52L$, $x_a^2 = 0.71L$, $x_n^1 = 0.3L$, $x_n^2 = 0.6L$, $\sigma_1 = 2.80106 \times 10^6 EI/L^3$, $\sigma_2 = -4.57068 \times 10^6 EI/L^3$, $\tau_1 = 4.93548 \times 10^5 EI/L$ and $\tau_2 = -7.75327 \times 10^6 EI/L$. For the dash–dotted line, $\sigma_1 = 1.79258 \times 10^4 EI/L^3$ and $\sigma_2 = 9.19000 \times 10^3 EI/L^3$. The attachment and node locations are not collocated.

Table 4
The vibration amplitudes of the sprung masses for different stiffnesses

k_1, k_2	k_{r1}, k_{r2}	m_1	m_2	z_1	z_2
1	5	1.3717E−03	1.3717E−03	3.6466E−04	9.4626E−01
15	10	2.0576E−02	2.0576E−02	2.4311E−05	6.3084E−02
20	30	2.7435E−02	2.7435E−02	1.8233E−05	4.7313E−02
50	45	6.8588E−02	6.8586E−02	7.2931E−06	1.8925E−02
100	80	1.3718E−01	1.3717E−01	3.6465E−06	9.4628E−03

The corresponding masses are also shown. The system parameters are $\omega = 27\sqrt{EI/(\rho L^4)}$, $x_f = 0.77L$, $x_a^1 = 0.52L$, $x_a^2 = 0.71L$, $x_n^1 = 0.3L$, $x_n^2 = 0.6L$, $\sigma_1 = 2.80106 \times 10^6 EI/L^3$, $\sigma_2 = -4.57068 \times 10^6 EI/L^3$, $\tau_1 = 4.93548 \times 10^5 EI/L$ and $\tau_2 = -7.75327 \times 10^6 EI/L$. The attachment and node locations are not collocated. The stiffnesses k_i and k_{ri} of the springs are non-dimensionalized by dividing by EI/L^3 and EI/L, respectively. The masses m_i are non-dimensionalized by dividing by ρL. The displacements z_1 and z_2 of the oscillator masses are non-dimensionalized by dividing by L.

and the vibration in the region between 0 and $0.4L$ is substantially quenched. Moreover, note that when a node or fixed node is imposed, the left end of the beam resembles a fixed boundary condition, even though the physical boundary condition is simply supported.

Now consider the case of enforcing two fixed nodes. A harmonic excitation with $\omega = 27\sqrt{EI/(\rho L^4)}$ is applied at $x_f = 0.77L$. Two sets of oscillators (each set consists of a sprung mass and a rotational oscillator) are attached at $x_a^1 = 0.52L$ and $x_a^2 = 0.71L$ for the purpose of inducing fixed nodes at $x_n^1 = 0.3L$ and $x_n^2 = 0.6L$. Solving Eqs. (23) and (24) gives $\sigma_1 = 2.80106 \times 10^6 EI/L^3$, $\sigma_2 = -4.57068 \times 10^6 EI/L^3$, $\tau_1 = 4.93548 \times 10^5 EI/L$ and $\tau_2 = -7.75327 \times 10^6 EI/L$. To impose nodes whereby only sprung masses are attached [11], one finds $\sigma_1 = 1.79258 \times 10^4 EI/L^3$ and $\sigma_2 = 9.19000 \times 10^3 EI/L^3$. In Fig. 10 is shown the deformed shape of the beam. Note that the beam with two nodes (see the dash–dotted line) remains motionless in the region between 0 and $0.6L$, while the beam with two fixed nodes (see the solid line) remains nearly stationary in the range between 0 and $0.72L$. Thus, the region of zero displacement is wider for the beam carrying translational and rotational oscillators compared to the beam carrying sprung masses only. Moreover, note that the vibration at any point along the beam with fixed nodes is lower than the vibration of the beam with nodes only. Nevertheless, depending on applications, attaching properly tuned spring–mass

Table 5
The vibration amplitudes of the rotational oscillators for different stiffnesses

k_1, k_2	k_{r1}, k_{r2}	I_1	I_2	θ_1	θ_2
1	5	6.8588E−03	6.8587E−03	2.3135E−06	8.6410E−03
15	10	1.3718E−02	1.3717E−02	1.1568E−06	4.3205E−03
20	30	4.1155E−02	4.1152E−02	3.8557E−07	1.4402E−03
50	45	6.1734E−02	6.1728E−02	2.5704E−07	9.6011E−04
100	80	1.0976E−01	1.0974E−01	1.4457E−07	5.4007E−04

The corresponding inertias are also shown. The system parameters are $\omega = 27\sqrt{EI/(\rho L^4)}$, $x_f = 0.77L$, $x_a^1 = 0.52L$, $x_a^2 = 0.71L$, $x_n^1 = 0.3L$, $x_n^2 = 0.6L$, $\sigma_1 = 2.80106 \times 10^6 EI/L^3$, $\sigma_2 = -4.57068 \times 10^6 EI/L^3$, $\tau_1 = 4.93548 \times 10^5 EI/L$ and $\tau_2 = -7.75327 \times 10^6 EI/L$. The attachment and node locations are not collocated. The stiffnesses k_i and k_{ri} of the springs are non-dimensionalized by dividing by EI/L^3 and EI/L, respectively. The inertias I_i are non-dimensionalized by dividing by ρL^3.

systems may often be sufficient to suppress the vibration to an acceptable level if the node and attachment locations are strategically chosen.

In Tables 4 and 5 are given the mass and inertia amplitudes for the translational and rotational oscillators of Fig. 10 for different sets of k_i and k_{ri} values. For convenience, $k_1 = k_2$ and $k_{r1} = k_{r2}$. For the σ_i and τ_i of Fig. 10, the mass and inertia parameters can be readily determined once the stiffnesses are specified, whose bounds are given by Eqs. (26) and (27). For the system parameters of Fig. 10, because the σ_i and τ_i are so large, for the stiffness values shown in Tables 4 and 5, $m_1 \approx m_2$ and $I_1 \approx I_2$. Moreover, from Tables 4 and 5, note that the vibration amplitude of each oscillator decreases with increasing stiffness. Interestingly, for each translational and rotational oscillator, the products of $m_i z_i$ and $I_i \theta_i$ remain unchanged, same as the results found in Ref. [12] where only nodes are imposed. For the system parameters of Fig. 10, $m_1 z_1 = 5.0022\text{E}-07 F\rho L^4/(EI)$, $m_2 z_2 = 1.2980\text{E}-03 F\rho L^4/(EI)$, $I_1\theta_1 = 1.5868\text{E}-08 F\rho L^5/(EI)$ and $I_2\theta_2 = 5.9266\text{E}-05 F\rho L^5/(EI)$. Like the collocated case, once the products $m_i z_i$ and $I_i\theta_i$ have been determined, the oscillator parameters can be selected to satisfy the maximum allowable amplitudes for the masses and inertias.

In application, the attachment locations for the translational and rotational oscillators do not have to coincide. It is easy to extend our results to impose fixed points by attaching multiple translational and rotational oscillators at distinct locations along the beam. In this case, Eqs. (23) and (24) become

$$\boldsymbol{\phi}^{\mathrm{T}}(x_n^r)\left\{[K^d] + \sum_{i=1}^{S}[\sigma_i \boldsymbol{\phi}(x_{at}^i)\boldsymbol{\phi}^{\mathrm{T}}(x_{at}^i) + \tau_i \boldsymbol{\phi}'(x_{ar}^i)\boldsymbol{\phi}'^{\mathrm{T}}(x_{ar}^i)] - \omega^2[M^d]\right\}^{-1} F\boldsymbol{\phi}(x_f) = 0, \tag{29}$$

$$\boldsymbol{\phi}'^{\mathrm{T}}(x_n^r)\left\{[K^d] + \sum_{i=1}^{S}[\sigma_i \boldsymbol{\phi}(x_{at}^i)\boldsymbol{\phi}^{\mathrm{T}}(x_{at}^i) + \tau_i \boldsymbol{\phi}'(x_{ar}^i)\boldsymbol{\phi}'^{\mathrm{T}}(x_{ar}^i)] - \omega^2[M^d]\right\}^{-1} F\boldsymbol{\phi}(x_f) = 0, \tag{30}$$

where x_{at}^i and x_{ar}^i designate the attachment locations of the ith translational and rotational oscillators, respectively. Solving Eqs. (29) and (30) simultaneously for the σ_i and τ_i, one can then choose the oscillator parameters to impose fixed nodes at the desired locations. To illustrate this more general case, consider a case where all the parameters are identical to those shown in Fig. 7, with the exception that the rotational oscillator is moved from $0.65L$ to $0.4L$ ($\omega = 57\sqrt{EI/(\rho L^4)}$, $x_f = 0.77L$, $x_{at} = 0.65L$, $x_{ar} = 0.4L$, and $x_N = 0.31L$). Eqs. (29) and (30) give $\sigma = 1.93531 \times 10^3 EI/L^3$ and $\tau = 9.86315 \times 10^3 EI/L$. To impose a node whereby only one sprung mass is attached [11] at $0.65L$, one finds $\sigma = 1.89511 \times 10^3 EI/L^3$. Fig. 11 shows the steady state lateral displacement of the beam. Note that a fixed node at $x_n = 0.31L$ is still induced, even though the attachment locations for the translational and rotational oscillators are different. While the lateral displacements of the beam in the region between $0.4L$ and $1.0L$ are higher than those shown in Fig. 7, the vibration of the beam between 0 to $0.4L$ is still substantially quenched. Thus, one can impose fixed nodes by attaching the translational and rotational oscillators at distinct locations.

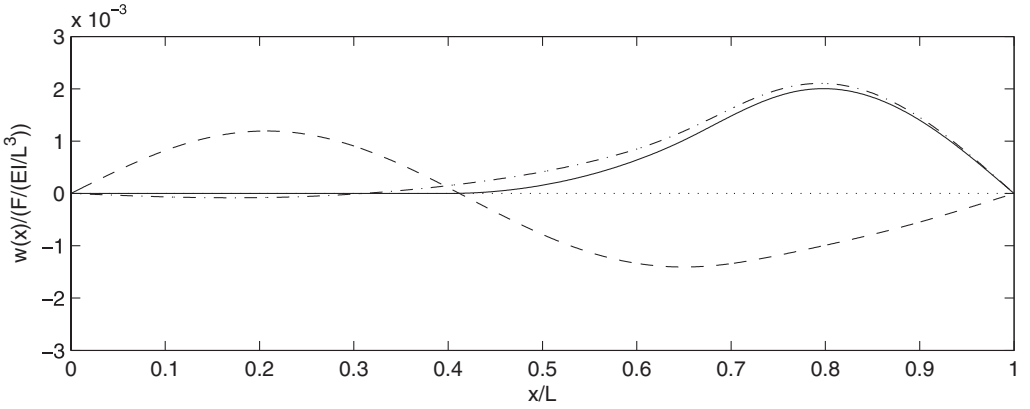

Fig. 11. The steady state deformed shapes of a uniform simply supported Euler–Bernoulli beam with a sprung mass as well as a rotational oscillator (solid line), with a sprung mass only (dash–dotted line), and without any oscillator (dashed line). The system parameters for the solid line are $\omega = 57\sqrt{EI/(\rho L^4)}$, $x_f = 0.77L$, $x_{at} = 0.65L$, $x_{ar} = 0.4L$, $x_n = 0.31L$, $\sigma = 1.93531 \times 10^3 EI/L^3$ and $\tau = 9.86315 \times 10^3 EI/L$. For the dash–dotted line, $\sigma = 1.89511 \times 10^3 EI/L^3$. The attachment and node locations are not collocated.

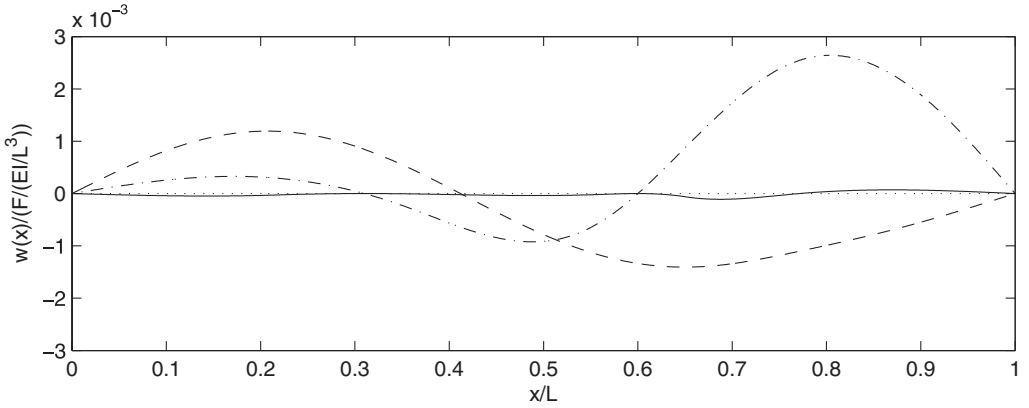

Fig. 12. The steady state deformed shapes of a uniform simply supported Euler–Bernoulli beam with two sprung masses as well as two rotational oscillators (solid line), with two sprung masses only (dash–dotted line), and without any oscillator (dashed line). The system parameters for solid line are $\omega = 27\sqrt{EI/(\rho L^4)}$, $x_f = 0.77L$, $x_{at}^1 = 0.35L$, $x_{at}^2 = 0.55L$, $x_{ar}^1 = 0.22L$, $x_{ar}^2 = 0.65L$, $x_n^1 = 0.31L$, $x_n^2 = 0.6L$, $\sigma_1 = -4.18674 \times 10^6 EI/L^3$, $\sigma_2 = 1.49858 \times 10^6 EI/L^3$, $\tau_1 = -6.10210 \times 10^1 EI/L$ and $\tau_2 = -2.81142 \times 10^1 EI/L$. For the dash–dotted line, $\sigma_1 = 5.72604 \times 10^3 EI/L^3$ and $\sigma_2 = -4.01197 \times 10^3 EI/L^3$. The attachment and node locations are not collocated.

As the last example, consider now a case where two translational and two rotational oscillators are employed to obtain two fixed points at $x_n^1 = 0.31L$ and $x_n^2 = 0.6L$. The attachment locations for the translational oscillators are $x_{at}^1 = 0.35L$ and $x_{at}^2 = 0.55L$, and the attachment locations of the rotational oscillators are $x_{ar}^1 = 0.22L$ and $x_{ar}^2 = 0.65L$. A harmonic excitation with frequency $57\sqrt{EI/(\rho L^4)}$ is applied at $x_f = 0.77L$. By solving Eqs. (29) and (30), one obtains $\sigma_1 = -4.18674 \times 10^4 EI/L^3$, $\sigma_2 = 1.49858 \times 10^4 EI/L^3$, $\tau_1 = -6.10210 \times 10^1 EI/L$ and $\tau_2 = -2.81142 \times 10^1 EI/L$. To impose two nodes with sprung masses attached at x_{at}^1 and x_{at}^2, one finds $\sigma_1 = 5.72604 \times 10^3 EI/L^3$ and $\sigma_2 = -4.01197 \times 10^3 EI/L^3$. In Fig. 12 is shown the steady state lateral displacement of the beam. Note that the vibration of the entire beam is drastically quenched after two fixed points are imposed.

By using the assumed modes method, a simple and efficient approach has been developed to solve the inverse problem of imposing one or more fixed nodes, or points of zero displacements and zero slopes, anywhere along an arbitrarily supported linear structure during harmonic excitations. This has practical

benefits because it allows any point along the structure to remain stationary without using any rigid supports, and it enables certain regions of the structure to undergo very small deflections, effectively quenching vibration in those sections.

4. Conclusions

Elastically mounted masses and rotational oscillators can be used to impose a single or multiple fixed nodes on any linear structure during harmonic excitations. When the parameters of the sprung masses and rotational oscillators are properly chosen, fixed nodes can always be induced at the attachment locations for any excitation frequency and excitation location. When the attachment and the fixed node locations are not collocated, it is only possible to induce a fixed node or multiple fixed nodes at certain locations along the structure. In addition, if the fixed node locations are properly selected, a region of nearly zero amplitudes can be imposed along the elastic structure for a given localized harmonic force without using any rigid supports, effectively quenching vibration in that segment of the structure. A detailed procedure to assist in the selection of the attached sprung masses and rotational oscillators was outlined, and bounds for the stiffnesses were given that serve as a design guide. Numerical experiments validated the utility of the proposed scheme of imposing a single or multiple fixed nodes during harmonic excitations for the collocated and non-collocated cases.

References

[1] R.G. Jacquot, Optimal dynamic vibration absorbers for general beam systems, *Journal of Sound and Vibration* 60 (4) (1978) 535–542.
[2] H.N. Özgüven, B. Çandir, Suppressing the first and second resonances of beams by dynamic vibration absorbers, *Journal of Sound and Vibration* 111 (3) (1986) 377–390.
[3] D.N. Manikanahally, M.J. Crocker, Vibration absorbers for hysteretically damped mass-loaded beams, *Journal of Vibration and Acoustics* 113 (1991) 116–122.
[4] R.F. Keltie, C.C. Cheng, Vibration reduction of a mass-loaded beam, *Journal of Sound and Vibration* 187 (2) (1995) 213–228.
[5] K. Alsaif, M.A. Foda, Vibration suppression of a beam structure by intermediate masses and springs, *Journal of Sound and Vibration* 256 (4) (2002) 629–645.
[6] L. Zuo, S.A. Nayfeh, Minimax optimization of multi-degree-of-freedom tuned-mass dampers, *Journal of Sound and Vibration* 272 (3–5) (2004) 893–908.
[7] M. Yaman, S. Sen, The analysis of the orientation effect of non-linear flexible systems on performance of the pendulum absorber, *International Journal of Non-Linear Mechanics* 39 (5) (2004) 741–752.
[8] M.B. Ozer, T.J. Royston, Application of Sherman–Morrison matrix inversion formula to damped vibration absorbers attached to multi-degree of freedom systems, *Journal of Sound and Vibration* 283 (3–5) (2004) 1235–1249.
[9] P.D. Cha, C. Pierre, Imposing nodes to the normal modes of a linear elastic structure, *Journal of Sound and Vibration* 219 (4) (1998) 669–687.
[10] P.D. Cha, Specifying nodes at multiple locations for any normal mode of a linear elastic structure, *Journal of Sound and Vibration* 250 (5) (2002) 923–934.
[11] P.D. Cha, Imposing nodes at arbitrary locations for general elastic structures during harmonic excitations, *Journal of Sound and Vibration* 272 (2004) 853–868.
[12] P.D. Cha, Enforcing nodes at required locations in a harmonically excited structure using simple oscillators, *Journal of Sound and Vibration* 279 (2005) 799–816.
[13] L. Meirovitch, *Analytical Methods in Vibrations*, Macmillan, New York, 1967.